

Hopping ionic conductivity in Ce-doped SrF₂.

II. Results obtained from impedance measurements

P. Dorenbos, H. W. den Hartog, R. Kruizinga, and S. Vrind

Solid State Physics Laboratory, University of Groningen, 1 Melkweg, 9718 EP Groningen, The Netherlands

(Received 31 July 1986)

The complex dielectric constant of Sr_{1-x}Ce_xF_{2+x} single crystals has been measured at frequencies between 90 Hz and 30 kHz with the temperature ranging from 100 to 550 K and 0.0001 < x < 0.40. We have paid special attention to the frequency and temperature dependence of the ionic conductivity. For Ce concentrations lower than 0.5 mol % frequency-independent Arrhenius-type ionic conductivity has been observed, which is attributed to the mobility of interstitial F⁻ ions dissociated from Ce³⁺-F⁻ dipolar complexes present in the crystals. At higher Ce concentration an increase of the ionic conductivity by several orders of magnitude has been observed; in addition the ionic conductivity depends upon the frequency. Employing a model in which the mobility of the interstitial F⁻ ions is relatively large in the vicinity of the Ce impurities and the Ce³⁺ ions are randomly distributed over the SrF₂ lattice the results have been interpreted. Essential in the interpretation is the random potential energy barrier structure in the crystals experienced by a hopping interstitial F⁻ ion.

I. INTRODUCTION

In Ref. 1 we have presented ionic thermocurrent (ITC) results obtained for single crystals of Sr_{1-x}Ce_xF_{2+x}. From these results conclusions have been drawn regarding the defect structure and the ionic conductivity. Additional information can be obtained by measuring the complex dielectric constant of the crystals ($\epsilon^* = \epsilon' - i\epsilon''$). The imaginary part of ϵ^* is proportional to the ionic conductivity (σ); $\epsilon'' = \sigma/\omega\epsilon_0$, where ω is the angular frequency and ϵ_0 is the dielectric permittivity of vacuum.

Most of the dielectric experiments performed on rare-earth-metal-doped fluorites, reported during the past ten years, have been carried out in order to reveal the defect structure of these fluorites. The attention has been focused mainly on the relaxation peaks observed in the dielectric spectra.²⁻⁷ Much less attention has been paid to the complex dielectric constant of the crystals at temperatures where the bulk ionic conductivity is the dominant property. Andeen *et al.*⁴ have observed this ionic conductivity contribution in the high-temperature part of the ϵ'' versus T plot of rare-earth-doped calcium fluoride, but this part of the spectrum has not been analyzed in detail. In more recent papers Fontanella *et al.*⁸ and Figueroa *et al.*⁹ have presented results obtained with impedance measurements performed on cubic lead fluoride doped with monovalent cations. These results pertain to relaxation peaks as well as to the bulk ionic conductivity. The bulk ionic conductivity in these materials behaves in accordance with the frequency-independent Arrhenius equation

$$\sigma = \frac{\sigma_0}{T} \exp \left[\frac{-E}{k_B T} \right], \quad (1)$$

where E is the activation energy and k_B is Boltzmann's constant. In Ref. 1 we have also found that an

Arrhenius-type ionic conductivity is present in SrF₂ doped with Ce concentrations smaller than 0.5 mol %. At higher concentrations, however, the ionic conductivity is expected to be frequency dependent. This frequency dependence has been studied recently by Welsh¹⁰ for CaF₂ crystals doped with 0.05 and 0.5-mol % YbF₃. These experiments were performed at a fixed temperature between 350 and 400 K and variable frequency ranging from 0.01 Hz to 100 kHz. We will present, in this paper, the complex dielectric constant of Sr_{1-x}Ce_xF_{2+x} as obtained from impedance measurements, which have been performed as a function of temperature at fixed frequencies (90 Hz, 300 Hz, 1 kHz, 3 kHz, 10 kHz, 30 kHz). The same crystals have been used as in the ionic thermocurrent experiments presented in Ref. 1.

We will conclude from our results that the bulk ionic conductivity and the dielectric constant of Ce-doped SrF₂ are strongly related to the inhomogeneity of the defect structure. This inhomogeneity appears to be very large for Ce concentrations of about 3-4 mol %. The bulk ionic conductivity at these concentrations can be described by a hopping mechanism, in which interstitial F⁻ ions migrate through the lattice by jumping over the random potential energy barriers present in the crystals.

II. EXPERIMENTAL PROCEDURES AND METHOD OF EVALUATION

With a General Radio 1615A capacitance bridge three terminal impedance measurements at six audio frequencies (90 Hz, 300 Hz, 1 kHz, 3 kHz, 10 kHz, 30 kHz) have been performed. In the sample holder, the crystal is placed between electrodes insulated by 0.7-mm-thick sapphire discs [see Fig. 1(a)]. The temperature of the sample holder can be varied between 80 and 550 K; the error in the temperature measurements is typically 3 K.

Because the dielectric properties of the sapphire discs

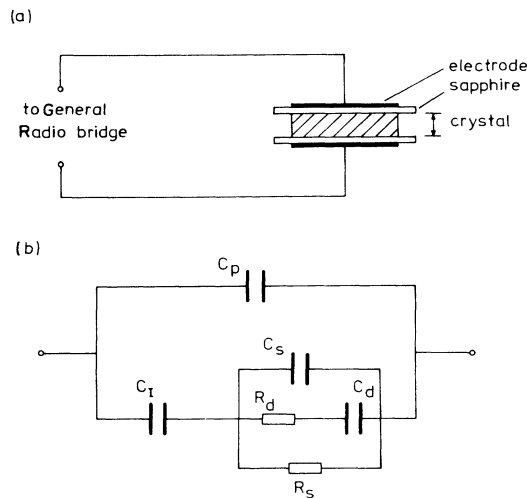


FIG. 1. (a) Drawing of the sample cell used for the impedance measurements, and (b) equivalent circuit used for the calculation of the crystal admittance.

are well known, the crystal admittance (Y^*) can be calculated from the measured total sample-cell impedance. To do so the sample cell is represented by a combination of resistances and capacitors; see Fig. 1(b). The sapphire discs have here been represented by C_I . C_p is a small capacitor parallel to the sample cell and is due to the capacitance between the wires leading to the electrodes (C_p is typically 0.1 pF). The crystal admittance is in series with C_I . Dielectric measurements with a configuration as shown in Fig. 1(b) have been discussed in detail by Müller.¹¹ The complex dielectric constant can be obtained straightforwardly from the crystal admittance ($Y^* = i\omega\epsilon^*\epsilon_0 A/d$). In the determination of ϵ^* we have not taken account the fringing field effects; this may introduce a systematic error in the real part of the dielectric constant. In the special case where dipole relaxations, obeying the Debye equations, and bulk ionic conductivity are present, the dielectric constant can be written as

$$\epsilon^* = \left[\epsilon(\infty) + \frac{\epsilon(0) - \epsilon(\infty)}{1 + (\omega\tau)^2} \right] - i \left[\frac{[\epsilon(0) - \epsilon(\infty)]\omega\tau}{1 + (\omega\tau)^2} + \frac{\sigma}{\omega\epsilon_0} \right], \quad (2)$$

where τ is the dipole relaxation time, $\epsilon(0)$ is the static dielectric constant, and $\epsilon(\infty)$ is the high-frequency dielectric constant. $\epsilon(0) - \epsilon(\infty)$ is the increase in the dielectric constant due to polarization of the nearest-neighbor (NN) dipoles and is equal to $N_d\mu^2/3k_B T\epsilon_0$. The admittance of the crystal can be represented by a capacitance C_s parallel to a resistance R_s and parallel to a series combination of C_d and R_d [Fig. 1(b)]. C_s is due to the instantaneous polarization and is proportional to $\epsilon(\infty)$. R_s is inversely proportional to the ionic conductivity and C_d is proportional to $\epsilon(0) - \epsilon(\infty)$, representing the dipole contribution to the crystal admittance. $R_d C_d$ is equal to the dipole relaxation time τ .

If an experiment is performed with sapphire discs between the electrodes and the crystal, the imaginary part of the complex capacitance of the sample cell shows the same features as an ITC recording. We have plotted in Fig. 2(a) this imaginary part for a sample cell containing a SrF_2 crystal doped with 0.76-mol % CeF_3 . The peak located at a temperature of 235 K corresponds with the NN dipole relaxation peak, which is observed at 152 K in ITC recordings.¹ The peak located around 500 K corresponds with the high-temperature (HT) peak observed in ITC recordings. The conductivity calculated from the results in Fig. 2(a) has been plotted in Fig. 2(b). At sufficiently high temperatures ($T > 400$ K) the bulk ionic conductivity dominates over the contribution originating from NN dipole relaxations. At lower temperatures ($1/T = 4.2 \times 10^{-3} \text{ K}^{-1}$) the NN dipole relaxation peak can be seen. Because we have treated the dipole peak extensively in Ref. 1 we will not discuss the NN dipole relaxation peak here in detail. In this paper we will concentrate our attention on the ionic conductivity.

In addition to the impedance measurements with sapphire discs we have also performed measurements in which the crystal surfaces had been painted with conducting silver paint. The interfacial capacitance (C_I), caused by the blocking electrodes, is in this case much larger

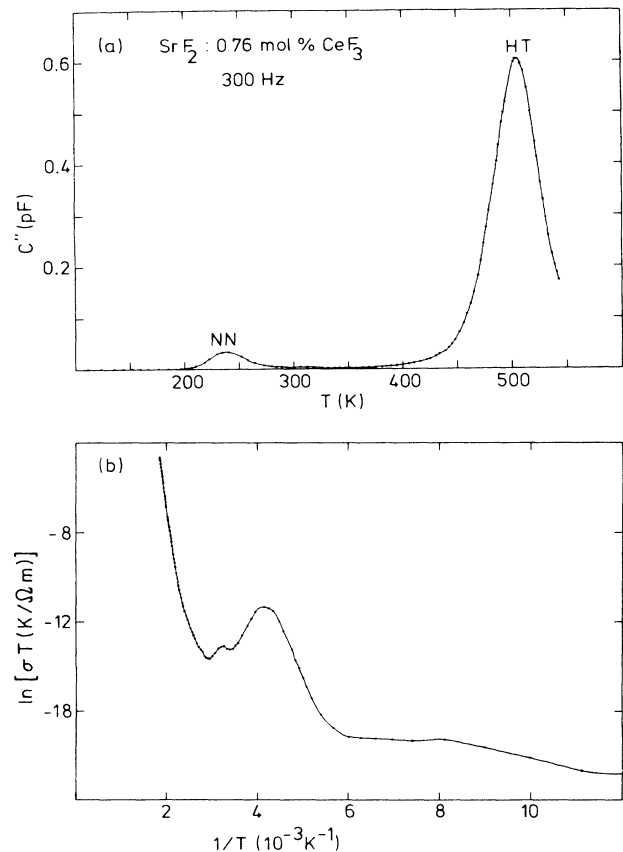


FIG. 2. (a) Imaginary part of the complex capacitance of the sample cell with a SrF_2 crystal doped with 0.76-mol % CeF_3 . (b) The calculated conductivity from the results in (a).

(≈ 10 nF) than when sapphire discs are used (≈ 3 pF). In this way it is possible to measure conductivities approximately two powers of ten larger than measurements with the use of sapphire discs. Because the exact value of the interfacial capacitance is not known, we cannot correct the measured sample-cell impedance for the presence of C_I in order to calculate the crystal admittance, only a correction for the small capacitance C_p can be made. It should, therefore, be kept in mind that the presented dielectric properties of the studied crystals may deviate from the true dielectric properties, especially if high conductivities are involved. This has been expressed by Eq. (3), which relates the true dielectric properties of the crystal (ϵ_s and σ_s) to the presented dielectric properties (ϵ^*):

$$\epsilon^* = \epsilon_s + \frac{d}{A\epsilon_0} \frac{C_I}{1 + i\omega \frac{d}{\sigma_s A} C_I} \quad (3)$$

In the derivation of (3) we have used that $C_I \gg C_s$. If the conductivity σ_s is small we obtain $\epsilon^* = \epsilon_s - i\sigma_s/\omega\epsilon_0$ and the presented results agree with the true crystal dielectric constant.

For large conductivities, ϵ^* deviates from the true complex dielectric constant caused by the interfacial polarization. From the measured sample-cell impedance we have estimated that the value of C_I is 10 nF. Inserting this value for C_I along with reasonable values for the thickness (d) and the surface area (A) of the crystal in Eq. (3) we find that as long as $\sigma \leq 10^{-9}\omega \Omega^{-1}\text{m}^{-1}$, ϵ' does not deviate more than 1% from ϵ_s and as long as $\sigma \leq 10^{-7}\omega \Omega^{-1}\text{m}^{-1}$ the presented conductivities do not deviate more than 1% from the true conductivity of the crystal.

III. EXPERIMENTAL RESULTS

The ionic conductivity measured for SrF_2 single crystals doped with 0.014-, 0.76-, 2.0-, 3.8-, 6.3-, 14-, and 37-mol % CeF_3 , have been plotted in Fig. 3. The results have been obtained from the impedance of the sample-cell with sapphire discs between the crystal surfaces and the electrodes. We have also included in Fig. 3 the conductivity calculated [employing Eq. (6) in Ref. 1] from the HT peak observed in the ITC recording of the 0.014-mol %-doped crystal. The essential difference between an ITC experiment and the impedance measurements is the low effective measuring frequency in ITC experiments (typically 0.01 Hz). In fact, the ITC results in Fig. 3 can be considered as the bulk dc ionic conductivity. It has been discussed in Ref. 1 that for Ce concentrations lower than 0.5 mol % the ionic conductivity is caused by the migration of interstitial F^- ions dissociated from $\text{Ce}^{3+}\text{-F}^-$ dipolar complexes. In this dilute concentration region the bulk ionic conductivity can be described by the Arrhenius equation [Eq. (1)]. We have constructed in Fig. 3 a straight line through the high-temperature data points of the results obtained from the impedance measurements and the ITC results; this line represents the bulk dc ionic conductivity. The conductivity observed at the right-hand side of this line is attributed to other processes. The major contribution comes from the dipole relaxation peak. In order to illustrate this contribution we have sketched in

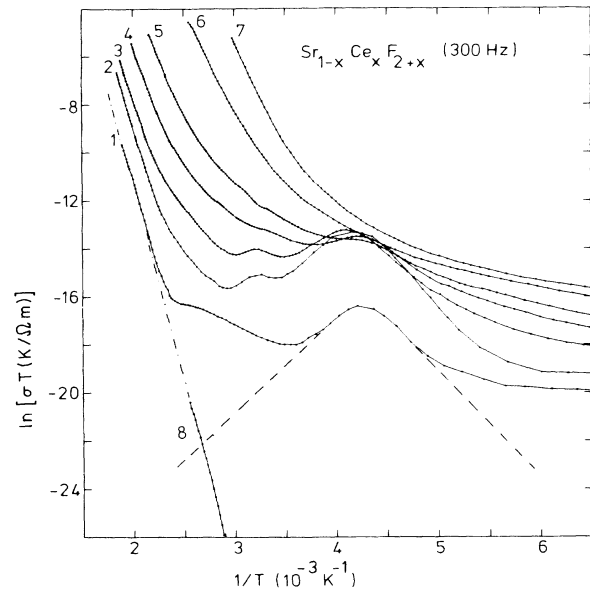


FIG. 3. Survey of the conductivity of $\text{Sr}_{1-x}\text{Ce}_x\text{F}_{2+x}$ for various Ce concentrations at a frequency of 300 Hz. (1) $x=0.00014$; (2) $x=0.0076$; (3) $x=0.02$; (4) $x=0.038$; (5) $x=0.063$; (6) $x=0.14$; (7) $x=0.37$; (8) ITC results obtained for $x=0.00014$. The dash-dotted line represents the dc ionic conductivity contribution and the dashed curve represents the contribution from NN dipole relaxations to the conductivity of the crystal with $x=0.00014$.

Fig. 3 (dashed curve) the Debye curve, which gives an approximate description of the dipole relaxation peak. The conductance observed at the right-hand side of the Debye peak is caused mainly by a low-temperature relaxation; this relaxation can be observed at temperatures around 125 K in Fig. 2(b) for the 0.76-mol %-doped crystal. We will not discuss the origin of this relaxation peak in this paper; we remark only that at Ce concentrations higher than 5 mol % the peak disappears. The conductance observed at temperatures between the Debye peak and the dc ionic conductivity line can partially be attributed to the relaxation which causes the 193-K peak in the ITC recordings (see Ref. 1). The remaining part of the conductivity is attributed to ac ionic conductivity and will be discussed in the following sections of this paper.

The conductivity measured for the 0.76-mol %-doped crystal can be interpreted in the same way as has been done for the 0.014-mol %-doped crystal. Again a Debye contribution from NN dipolar $\text{Ce}^{3+}\text{-F}^-$ complexes and an Arrhenius-type ionic conductivity can be observed. The remaining ac ionic conductivity part, between the Debye contribution and the Arrhenius contribution to the total conductivity, is much larger than in the 0.014-mol %-doped crystal. At still higher concentrations no clear distinction between Arrhenius-type ionic conductivity and other contributions to the observed conductivity can be made. Instead a gradual change from a strongly temperature-dependent conductivity observed at high temperatures to very weak temperature-dependent conductivity at low temperatures has been observed for the 14- and

the 37-mol %-doped crystals. Apart from the relaxation peaks, the conductivity of the crystals increases with the Ce concentration. This increase is rather drastic at high temperatures, but is observed at low temperatures too, although much less pronounced (e.g., the dc conductivity increases from $3.4 \times 10^{-15} \Omega^{-1}\text{m}^{-1}$ at $1/T = 3 \times 10^{-3}$ for the 0.014-mol %-doped crystal to $1.5 \times 10^{-5} \Omega^{-1}\text{m}^{-1}$ for the 37-mol %-doped crystal; an increase of almost 10 orders of magnitude).

In order to make a clear distinction between a dc and an ac contribution to the total conductivity, impedance measurements as a function of the frequency have been performed. For these measurements painted silver electrodes have been used. In Figs. 4(a) and 4(b) the conductivity and the real part of the dielectric constant of SrF_2 doped with 0.4-mol % CeF_3 at six distinct frequencies have been presented. The frequency-independent character of the Arrhenius-type ionic conductivity, observed at high temperatures, can be observed clearly. We have also included in Fig. 4(a) the conductivity, calculated from the HT peak of the ITC recording obtained for the same crystal.

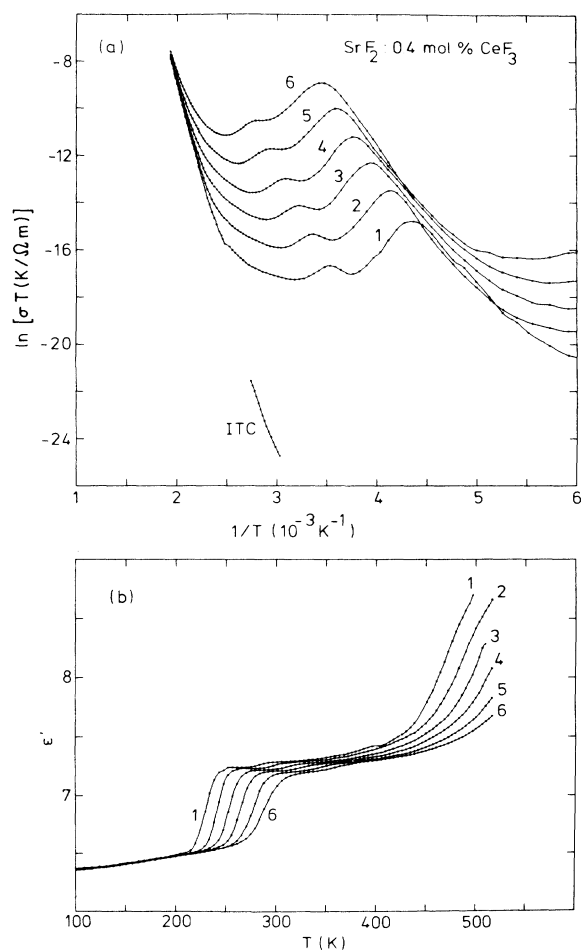


FIG. 4. (a) Conductivity plots and (b) $\epsilon'(T)$ plots obtained for a 0.4-mol % CeF_3 -doped SrF_2 crystal at six distinct frequencies. Curve 1, $\nu = 90$ Hz; 2, $\nu = 300$ Hz; 3, $\nu = 1$ kHz; 4, $\nu = 3$ kHz; 5, $\nu = 10$ kHz; 6, $\nu = 30$ kHz.

The value of ϵ' , measured with a frequency of 90 Hz, is approximately 6.4 at temperatures around 150 K [see Fig. 4(b)] and increases slowly with increasing temperature until the NN dipole relaxation peak starts to contribute. A jump in ϵ' , equal to $N_d \mu^2 / 3k_B T \epsilon_0$, can now be seen. At temperatures above 400 K, ϵ' increases to a value of ≈ 8.7 at 500 K. This increase cannot be caused by the interfacial polarization because the condition $\sigma < 10^{-9} \omega \Omega^{-1}\text{m}^{-1}$ holds, which implies that the interfacial polarization contributes less than 1% to the value of ϵ' . Instead it is associated with the dielectric properties of the bulk crystal.

In Figs. 5(a) and 5(b) the results obtained for SrF_2 doped with 4.8-mol % CeF_3 have been plotted. The small bumps in the $\ln(\sigma T)$ versus $1/T$ curves are caused by the $\text{Ce}^{3+}\text{-F}^-$ dipolar complexes. At high temperatures frequency-independent conductivity can be observed, whereas at low temperatures the conductivity depends very strongly upon the frequency. The small vertical bars in the $\epsilon'(T)$ curves [see Fig. 5(b)] indicate the points where the interfacial polarization starts to contribute more than

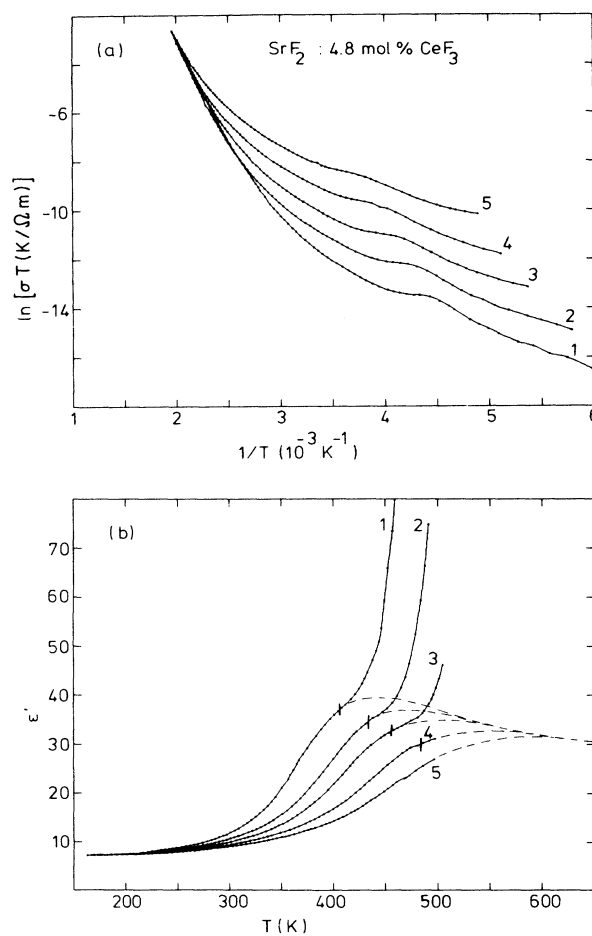


FIG. 5. (a) Conductivity plots and (b) $\epsilon'(T)$ plots obtained for a 4.8-mol % CeF_3 -doped SrF_2 crystal at five distinct frequencies. Curve 1, $\nu = 300$ Hz; 2, $\nu = 1$ kHz; 3, $\nu = 3$ kHz; 4, $\nu = 10$ kHz; 5, $\nu = 30$ kHz. The dashed curves represent possible $\epsilon'(\omega, T)$ curves without the contribution from the interfacial polarization.

1% to ϵ' . At temperatures higher than those associated with these bars the contribution of the interfacial polarization to ϵ' increases approximately quadratically with the conductivity. At lower temperatures the dielectric constant is determined by the properties of the studied crystal only. The $\epsilon'(T)$ curve measured at a frequency of 300 Hz increases from a value of 7.3 at a temperature of 200 K to a value of 35.5 at 400 K. It appears that ϵ' becomes constant at temperatures higher than 400 K; however, this is obscured by the presence of the interfacial contribution. The features observed for $\epsilon'(T)$ at a frequency of 300 Hz have also been observed for the other frequencies.

In Fig. 6 the results obtained for SrF_2 doped with 23 mol % CeF_3 have been plotted. Again a frequency-independent conductivity can be observed at high temperatures and a strongly frequency-dependent conductivity can be observed at low temperatures. The vertical bars in Fig. 6(b) serve the same purpose as those in Fig. 5(b).

IV. THEORY

The physical and theoretical background of the ionic conductivity observed in dilutely CeF_3 -doped SrF_2 crys-

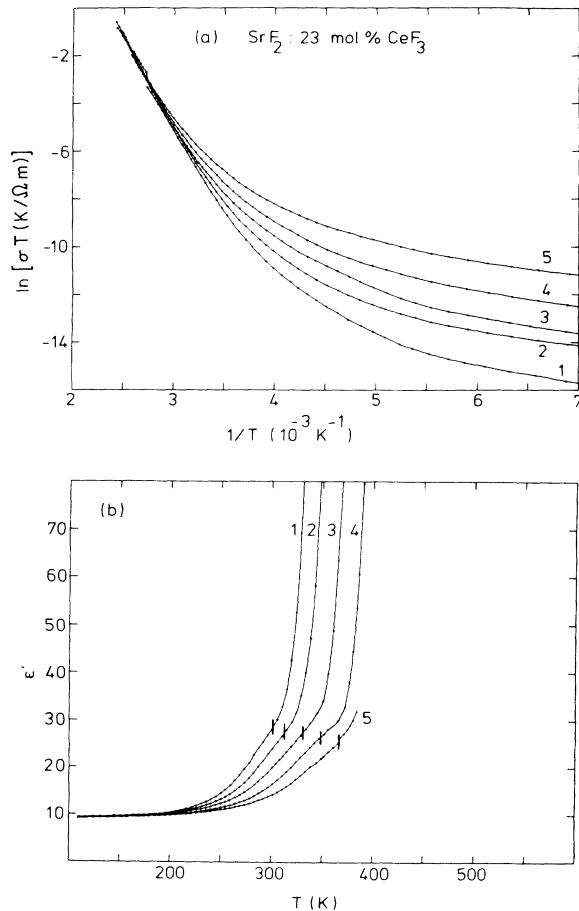


FIG. 6. (a) Conductivity plots and (b) $\epsilon'(T)$ plots obtained for a 23-mol % CeF_3 -doped SrF_2 crystal at five distinct frequencies. Curve 1, $\nu = 300 \text{ Hz}$; 2, $\nu = 1 \text{ kHz}$; 3, $\nu = 3 \text{ kHz}$; 4, $\nu = 10 \text{ kHz}$; 5, $\nu = 30 \text{ kHz}$.

tals is well understood by now. Interstitial F^- ions, dissociated from $\text{Ce}^{3+}\text{-F}^-$ dipolar complexes, hopping through the host material (SrF_2) will lead to an ionic conductivity obeying the Arrhenius equation. At higher Ce concentrations, however, the potential energy barriers experienced by a hopping interstitial F^- ion may vary from site to site and the ionic conductivity can no longer be described with the Arrhenius equation. Jonscher¹² has given a formal theoretical description of the conductivity caused by hopping of charge carriers in a random medium. We will apply this description to the crystals studied in this paper.

When $\text{Sr}_{1-x}\text{Ce}_x\text{F}_{2+x}$ is subject to a unit step function in the electric field, the interstitial F^- ions will respond by hopping from one interstitial site towards another one, also polarization of electrons, ions, as well as dipoles will be induced. From the Laplace transformation of the current response to the frequency domain, the complex dielectric constant can be obtained. The real and imaginary parts are related to each other through the Kramers-Kronig relations. The current density $J(t)$ can be written formally as

$$J(t) = \epsilon_0 \epsilon(\infty) \delta(t) + \sum_m \frac{qr_m}{dA} \delta(t - t_m), \quad (4)$$

where $\epsilon_0 \epsilon(\infty) \delta(t)$ is the instantaneous polarization; $(qr_m/dA) \delta(t - t_m)$ represents the contribution of a F^- hop at time t_m to the total current density; q is the F^- charge; r_m is the component of the displacement of the hopping ion along the direction of the electric field. The summation of all the individual F^- jumps, indexed by m , gives the total hopping current. For simplicity we have assumed that the flight time of a jump from one site towards another site is zero as compared to the time of one period of the measuring frequency; furthermore, we have assumed that there are no relaxation effects accompanying a single transition.¹²

Transformation of Eq. (4) to the frequency domain, and dividing by ϵ_0 , gives the dielectric constant

$$\epsilon^*(\omega) = \epsilon(\infty) + \sum_m \frac{qr_m}{d\epsilon_0 A} [\cos(\omega t_m) + i \sin(\omega t_m)]. \quad (5)$$

Equation (5) gives an explicit relation between the individual F^- hops and the capacitance and ionic conductivity of the doped SrF_2 crystals. If t_m is considered to be a continuous function of m then the relation between the current response $J(t)$ and the function $t(m)$ can be written as

$$J(t) = \frac{qr}{dA} \left[\frac{dt(m)}{dm} \right]^{-1}. \quad (6)$$

Because only the effective jumps along the direction of the electric field contribute to the hopping current, we have replaced r_m by r in Eq. (6).

If the hopping times have a uniform distribution in time, $t(m)$ increases linearly with the index m and $J(t)$ is then constant. A frequency-independent ionic conductivity and capacitance is now obtained. The Arrhenius conductivity observed in the dilute concentration region is an example of this type of ionic conductivity.

In a random medium the current density resulting from

a step function electric field excitation will not be constant. First the most mobile ions will respond, leading to a high current, just after the excitation. After some time these mobile ions encounter high potential energy barriers and the initial high ionic conductivity decreases until the dc conductivity remains. Translated to the frequency domain this means that at low frequencies the conductivity becomes frequency independent. An essential parameter is the time $1/\omega$ in relation to the time it takes to reach a steady-state current, which depends upon temperature because F^- jumps in SrF_2 are thermally activated. At high temperatures and/or low frequencies frequency-independent ionic conductivity and capacitance is expected to be observed. At higher frequencies and/or lower temperatures the conductivity and capacitance is expected to become frequency dependent. This frequency dispersion of the conductivity has been observed in many disordered materials in which the conductivity is caused by a hopping process of charge carriers, as has been demonstrated by Jonscher.¹²⁻¹⁵ The frequency-dependent bulk conductivity of these materials can be described by the empirical relation

$$\sigma(\omega) = a(T)\omega^{n(T)}, \quad (7)$$

where the exponent n is in the range $0 < n(T) < 1$ and depends upon the temperature. This power law can be observed over a large frequency interval; however, at very low frequencies dc ionic conductivity will be observed and $n = 0$. If Eq. (7) is transformed back to the time domain the current density, resulting from a unit step electric field excitation, is proportional to t^{-n} . This power-law dependence of the current density is known as the Curie-von Schweidler law.

V. DISCUSSION

In this paper we have presented the dielectric properties of $Sr_{1-x}Ce_xF_{2+x}$ as a function of the Ce concentration (x), the temperature (T), and the frequency. In order to interpret these results in a comprehensive way we will first give some general remarks regarding the dielectric properties and then discuss the results more in detail.

Because the defect structure of the crystals is essential for the interpretation of the observed dielectric properties, we will treat the results obtained for the dilutely ($x < 0.005$), the intermediately ($0.005 < x < 0.1$), and the heavily ($x > 0.1$) doped crystals separately. Once the defect structure has been discussed the temperature and the frequency dependence is interpreted.

The dependence of the dielectric properties upon the temperature can be caused by the following: (i) The defect structure of the crystals may change with the temperature, e.g., the dissociation of interstitial F^- ions from Ce^{3+} - F^- dipolar complexes. (ii) The hopping rate of an interstitial F^- ion from one site towards an adjacent site is thermally activated and depends exponentially upon $-1/T$. The contribution from these hopping ions to ϵ^* is, therefore, strongly temperature dependent, contrary to nonthermally activated contributions like the instantaneous polarization of the crystals.

The measuring frequency determines the time scale at

which the dielectric properties are studied. Only those charge carriers which respond within a time of approximately $1/\omega$ to the applied alternating electric field will contribute to ϵ^* . At very high frequencies only the instantaneous polarization contributes significantly, whereas at very low frequencies dc ionic conductivity can be observed.

A contribution to ϵ^* , which is always present, is the instantaneous polarization, caused by the polarizability of the ions and the electrons present in the crystals. This contribution, denoted by $\epsilon(\infty)$, can be observed at sufficiently high frequencies or sufficiently low temperatures if the NN dipoles do not contribute to ϵ^* . The value of $\epsilon(\infty)$ is determined by the concentration of charge carriers and their individual polarizabilities. Although we are, in this paper, interested mainly in the contribution from the hopping ions to the complex dielectric constant two remarks regarding the observed values of $\epsilon(\infty)$ are made: (i) It has been observed [e.g., Figs. 4(b), 5(b), and 6(b)], that at temperatures around 200 K ϵ' increases approximately linearly with the Ce concentration x ($\epsilon' \simeq 6.4 + 13x$). This is caused by the substitution of Sr^{2+} ions for Ce^{3+} ions, which possess a polarizability different from that of Sr^{2+} , and the higher density of the electrons and the ions in the doped crystals. (ii) In addition it has been observed in Fig. 4(b) that at temperatures around 150 K ϵ' increases $(1.36 \pm 0.02) \times 10^{-3}$ per degree Kelvin. This increase agrees with results obtained by Andeen *et al.*,¹⁶ and is caused mainly by the thermal expansion of the crystal; we refer to these authors for a more detailed description of this effect upon ϵ' .

A. The dilute concentration region

In Ref. 1 we have shown that the ITC results obtained for SrF_2 doped with CeF_3 concentrations smaller than 0.5 mol % can be explained by an Arrhenius-type ionic conductivity. With the results presented in this paper, obtained for SrF_2 doped with 0.014- and 0.4-mol %- CeF_3 (see Figs. 3 and 4) we can give more quantitative support for this explanation. From the slopes of the conductivity curves, plotted as $\ln(\sigma T)$ versus $1/T$, the activation energy E and the value of σ_0 , which have been compiled in Table I, can be obtained. We have also compiled the results obtained for a 0.1-mol %-doped crystal in Table I.

The activation energies for the 0.014-, 0.1-, and 0.4-mol %-doped crystals are within the measuring accuracy equal to each other. The mean value is (1.34 ± 0.02) eV. The value of σ_0 is determined by the concentration of dissociated F^- ions and should be proportional to the square

TABLE I. Ionic conductivity parameters of $Sr_{1-x}Ce_xF_{2+x}$.

x	E (eV)	σ_0 (10^8 K/ Ω m)
0.000 14	1.33 ± 0.03	8 ± 3
0.001	1.36 ± 0.03	58 ± 20
0.004	1.33 ± 0.03	33 ± 10
0.048	0.76 ± 0.04	0.03 ± 0.01
0.14	0.72 ± 0.04	0.5 ± 0.2
0.23	0.61 ± 0.04	0.12 ± 0.05

root of the Ce concentration x . However, because of the inaccuracy of the values for σ_0 this \sqrt{x} dependence cannot be observed clearly in Table I.

The correspondence between the results obtained with the impedance measurements and the results obtained from the HT peak observed in ITC recordings¹ has been demonstrated in Fig. 3. The ionic conductivity measured above 400 K at 300 Hz for the 0.014-mol % -doped crystal extrapolated towards lower temperatures, agrees with the conductivity calculated from the HT peak. This confirms the conclusion in Ref. 1 that the HT peak is caused by the ionic conductivity and not by bound charges as has been suggested by Laredo *et al.*¹⁷ The correspondence can also be observed in Fig. 4(a). The absolute value of the ionic conductivity obtained from the ITC recording, plotted in this figure agrees with the extrapolated conductivity calculated from the impedance measurements. The slopes of the $\ln(\sigma T)$ versus $1/T$ curves, however, do not agree with each other. In the calculation of the ionic conductivity from the HT peak we have assumed that the real part of the dielectric constant of the crystal remains constant with the temperature. This is, however, not the case, as can be observed in Fig. 4(b). The dielectric constant increases with the temperature and becomes frequency dependent. If only dc ionic conductivity is present in the crystal, ϵ' should be frequency independent, as can be derived from the Kramers-Kronig relations. We conclude, therefore, that there are more contributions to the complex dielectric constant than only the dc ionic conductivity. The increase of ϵ' with the temperature will result in a broadening of the HT peak. This broadening, which amounts to ≈ 4 K for the 0.4-mol % -doped crystal [see Fig. 2(b) in Ref. 1], is responsible for the deviations in the calculated conductivity. The origin of the increase of ϵ' will be discussed in the section where the interpretation of the results obtained for the intermediately doped crystals will be presented.

The low-temperature part of the ionic conductivity plot in Fig. 4(a) is dominated by the contribution from the NN dipole relaxations. The shift, the position, and the slope of the relaxation peak as a function of the temperature and the frequency can be explained quantitatively with the Debye equations [Eq. (2)], although deviations from the "true" Debye behavior may occur due to the dipole-dipole (or dipole-defect) interactions.¹⁸ Note that the appearance of an Arrhenius-type dc ionic conductivity along with a Debye-type relaxation peak, as in Fig. 4(a), can also be observed in other crystalline materials like Na-doped PbF_2 (Refs. 8 and 9) or Ca-doped LaF_3 (Ref. 19).

B. The intermediate concentration region

The defect structure in the intermediately doped SrF_2 crystals is quite different from the dilutely doped crystals. At intermediate Ce concentrations the possibility of interstitial F^- ions percolating from one Ce ion towards another Ce ion should be considered also. We will base the discussion on two assumptions: (i) The Ce ions are distributed randomly over the SrF_2 lattice. (ii) Interstitial F^- jumps within a sphere, surrounding a Ce ion, with a radius equal to the distance of a next-nearest-neighbor

(NNN) site to the Ce ion (5.02 Å) is "easy" as compared to jumps at larger distances. Although this last assumption gives a rather simplified view of F^- motion in the lattice our results can, nevertheless, be interpreted with these assumptions. If two or more Ce ions share, in this view, equal NNN sites an interstitial F^- ion can jump relatively easily in the statistical cluster formed by the Ce ions. The name "statistical cluster" has been chosen in order to distinguish these clusters from a preferential cluster, which is due mainly to some sort of attractive interaction between the rare-earth impurities.

The empirical power law Eq. (7) between the ionic conductivity and the frequency is expected to hold for crystals with an intermediate CeF_3 concentration. We have, therefore, plotted in Fig. 7 the $\log(\sigma)$ versus $\log(\omega)$ curves, which have been derived from Fig. 5(a) obtained for SrF_2 crystals doped with 4.8-mol % CeF_3 . The slopes of the curves have been indicated in the figure and are equal to the parameter n in Eq. (7). We will first discuss the situation in which $n = 0$, which corresponds to dc ionic conductivity. This conductivity can be observed at high temperatures and/or low frequencies and is caused by the most difficult F^- jumps in the bulk crystal. From the tangential line which can be constructed through the high-temperature conductivity data in Fig. 5(a) the activation energy E and the value of σ_0 can be obtained; they have been compiled in Table I. It is, however, not possible to interpret these values as has been done in the dilutely doped crystals. The only conclusion we draw is that the value of E (0.76 eV) is some measure for the highest potential energy barriers present in the crystals; this value is lower than the potential energy barriers in pure SrF_2 (0.94 eV). It is further noted that σ_0 has decreased significantly as compared to values obtained for the dilutely doped crystals.

At temperatures lower than 500 K the ionic conductivity becomes frequency dependent and the value of n increases to 0.76 at a temperature of 300 K. Within the model of hopping ionic conductivity in a random medium

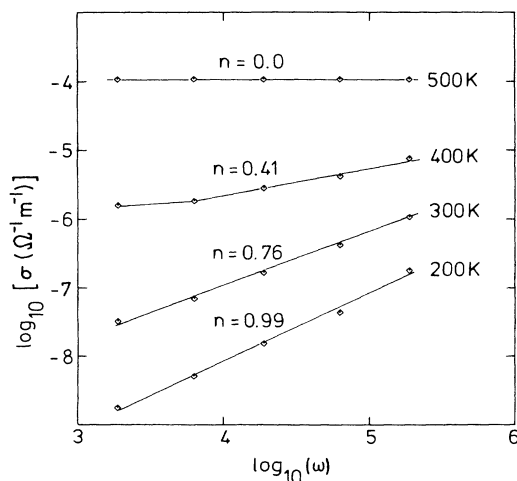


FIG. 7. $\log_{10}(\sigma)$ vs $\log_{10}(\omega)$ plots of SrF_2 doped with 4.8-mol % CeF_3 at several temperatures.

this ac ionic conductivity is caused by the hopping of F^- ions in areas of the crystal where the potential energy barriers are relatively low. If within a time of approximately $1/\omega$ the migration of these freely moving ions is not stopped by a high potential energy barrier, the F^- jumps will contribute mainly to σ and otherwise to ϵ' . The contribution to ϵ' will, therefore, increase as the frequency is decreased; this can be observed in Fig. 5(b). Because the jump rate of the interstitial F^- ions is thermally activated, the same holds if the temperature is increased. At very low frequencies and/or at high temperatures each F^- ion will encounter within a time of $1/\omega$ a high potential energy barrier, which must result in a leveling off of ϵ' ; at the same time the contribution to σ vanishes. What remains is the dc ionic conductivity caused by the "slower" jumps over the high potential energy barriers. In fact, the initial fast migration of the freely moving F^- ions in the statistical clusters becomes part of the instantaneous polarization of the crystal.

The leveling off of ϵ' was predicted eight years ago by Jonscher;¹⁵ however, very little experimental evidence regarding this leveling off was present at that time. We think that the onset of the predicted leveling off can be observed in our results. If the $\epsilon'(T)$ curve obtained with a frequency of 300 Hz is considered, it can be seen that at temperatures around 360 K ϵ' increases relatively sharply with the temperature; the slope of the curve is 0.34 K^{-1} . At a temperature of 410 K, around the position of the vertical bar, the slope of the $\epsilon'(T)$ curve is much less ($d\epsilon'/dT = 0.18 \text{ K}^{-1}$), and this is probably the onset to the leveling off of ϵ' at higher temperatures. Unfortunately, a constant value of ϵ' can not be observed due to the interfacial polarization, which at temperatures higher than 410 K start to contribute significantly to ϵ' . It seems that at higher frequencies than 300 Hz, and consequently higher temperatures, the leveling off occurs at lower values of ϵ' ; this can be understood with the Curie $1/T$ law, which decreases the polarization of the statistical clusters as the temperature increases.

At temperatures where the dc ionic conductivity can be observed, ϵ' must be frequency independent. With this in mind, and the Curie $1/T$ law, we have sketched in Fig. 5(b) the possible $\epsilon'(\omega, T)$ curves without the contribution from the interfacial polarization. We do not claim that these curves represent the true values; the only purpose is to illustrate the contribution to ϵ' from the easily polarizable F^- ions within the framework of the above discussed ionic conductivity model.

The low temperature ($\approx 200 \text{ K}$) results, where the value of n is almost equal to 1, will be discussed now. At these temperatures, well below the position of the NN relaxation peak, the hopping rate of interstitial F^- ions will be very low. Hopping ionic conductivity is, therefore, not the most probable explanation for the observed conductivity at these temperatures. Instead a nonthermally activated polarization process, leading to almost temperature-independent dielectric properties, is more likely. Results with a value of n close to 1 have been observed for a wide range of materials. The observations pertain to the conductivity at low temperatures as well as to the high-frequency part of dielectric loss peaks.¹⁴ The

results have been explained in the last couple of years by a nonthermally activated collective rearrangement of the charge carriers, caused by many-body interactions. We will not discuss this further in this paper, but we refer to Jonscher *et al.*^{12,20-24} who have considered the possibility of the many-body interactions and to the quantum mechanical theory developed by Dissado and Hill.^{25,26}

C. The concentrated concentration region

Many of the features observed for the intermediately doped crystals (see Fig. 5) are also observed for the heavily doped crystals (see Fig. 6). From the dc ionic conductivity measured at high temperatures for SrF_2 crystals doped with 23 mol % the parameters E and σ_0 have been obtained. These results, together with results obtained for SrF_2 doped with 14 mol % (not presented in this paper), have been compiled in Table I. E decreases with the Ce concentration, whereas σ_0 is small as compared to the results obtained for the dilutely doped crystal. The decrease of E should, within the model presented in this paper, be interpreted as a lowering of the highest potential energy barriers, caused by the decrease of the mean distance between the Ce ions.

At Ce concentrations above 10 mol % we can no longer describe the defect structure of the crystals in terms of isolated Ce ions and Ce ions involved in a statistical cluster. Instead almost all Ce ions are part of the "infinite" cluster. However, within this cluster randomness will still be present and interstitial F^- ions in easily conducting areas of the crystal will contribute to the ac ionic conductivity observed in Fig. 6. On purely statistical arguments we expect that the randomness in the heavily doped crystals is less than in the vicinity of the percolation threshold. As a result we also expect that the contribution from easily jumping F^- ions to ϵ' in the 23-mol %-doped crystal is less than in the 4.8-mol %-doped crystal. Unfortunately, this can not be concluded from the results in Fig. 6(b) due to the contribution from the interfacial polarization.

VI. SUMMARY

In this paper we have presented data concerning the defect structure and the hopping ionic conductivity in CeF_3 -doped SrF_2 . Due to the fact that preferential clustering of the Ce ions in SrF_2 seems to be rather unimportant, certainly as compared to rare-earth-doped CaF_2 and SrF_2 doped with the smaller rare-earth ions, the defect structure can be described by a random distribution of the Ce ions over the lattice.

In the dilutely Ce-doped crystals Arrhenius-type ionic conductivity, caused by interstitial F^- ions dissociated from the NN dipolar complexes, has been observed. From the activation energy obtained from the $\ln(\sigma T)$ versus $1/T$ curve, the dissociation energy of the dipolar complexes has been obtained. The results obtained with the ITC experiments are in accordance with the results obtained with the impedance measurements. Particularly, the HT peak observed in ITC recordings is caused by the

ionic conductivity of the bulk crystal and not by bound charges.

In the intermediately doped crystals the inhomogeneity of the defect structure plays an important role in the observed dielectric properties. The highest potential energy barriers determine the dc ionic conductivity. The height of these barriers decreases from 0.94 eV in pure SrF₂ to a value of $\cong 0.61$ eV in 23-mol % CeF₃-doped SrF₂. ac ionic conductivity has been observed at temperatures below the onset to the dc ionic conductivity, along with a frequency-dependent contribution to the real part of the complex dielectric constant. We have attributed this to easily conducting areas present in the random defect structure of the crystals. The increase of ϵ' , caused by the polarization of these easily conducting areas, is rather

large at concentrations around 4 mol %; here we expect a maximum randomness in the crystals. The broadening of the HT peak and the results obtained from the polarization experiments¹ can also be explained qualitatively with the increase of ϵ' .

We conclude this paper by emphasizing that we think that SrF₂ doped with the larger rare-earth ions (La, Ce, Pr, and Nd) are very suitable model materials to test theories about hopping ionic conductivity in random media, because (i) the interstitial positions, via which F⁻ ions can jump through the crystals, are well defined in the fluorite lattice, (ii) the Ce³⁺ ions seem to substitute randomly for the Sr²⁺ ions, and (iii) the inhomogeneity of the defect structure can be varied at will by varying the Ce concentration.

¹P. Dorenbos, S. Vrind, J. Dolfing, and H. W. den Hartog, preceding paper, Phys. Rev. B **35**, 5766 (1987).

²C. G. Andeen, J. J. Fontanella, M. C. Wintersgill, P. J. Welcher, R. J. Kimble, Jr., and G. E. Matthews, Jr., J. Phys. C **14**, 3557 (1981).

³J. Fontanella and C. Andeen, J. Phys. C **9**, 1055 (1976).

⁴C. Andeen, D. Link, and J. Fontanella, Phys. Rev. B **16**, 3762 (1977).

⁵A. Edgar and H. K. Welsh, J. Phys. C **8**, L336 (1975).

⁶A. Edgar and H. K. Welsh, J. Phys. C **12**, 703 (1979).

⁷H. W. den Hartog and J. Meuldijk, Phys. Rev. B **29**, 2210 (1984).

⁸J. J. Fontanella, M. C. Wintersgill, P. J. Welcher, A. V. Chadwick, and C. G. Andeen, Solid State Ionics **5**, 585 (1981).

⁹D. R. Figueroa, J. J. Fontanella, M. C. Wintersgill, A. V. Chadwick, and C. G. Andeen, J. Phys. C **17**, 4399 (1984).

¹⁰H. K. Welsh, J. Phys. C **18**, 5641 (1985).

¹¹P. Müller, Phys. Status Solidi A **67**, 11 (1981).

¹²A. K. Jonscher, J. Non-Cryst. Solids **8-10**, 293 (1972).

¹³A. K. Jonscher, *Dielectric Relaxations in Solids* (Chelsea

Dielectric Press, London, 1983).

¹⁴A. K. Jonscher, Nature **267**, 673 (1977).

¹⁵A. K. Jonscher, Philos. Mag. B **38**, 587 (1978).

¹⁶C. Andeen and D. Schuele, Phys. Rev. B **6**, 591 (1972).

¹⁷E. Laredo, N. Suarez, A. Bello, M. Puma, D. Figueroa, and J. Schoonman, Phys. Rev. B **32**, 8325 (1985).

¹⁸H. v. Weperen and H. W. den Hartog, Phys. Rev. B **18**, 2857 (1978).

¹⁹J. R. Igel, M. C. Wintersgill, J. J. Fontanella, A. V. Chadwick, C. G. Andeen, and V. E. Bean, J. Phys. C **15**, 7215 (1982).

²⁰A. K. Jonscher, Nature **250**, 191 (1974).

²¹A. K. Jonscher, Nature **253**, 717 (1975).

²²A. K. Jonscher, Phys. Status Solidi B **83**, 585 (1977); **84**, 159 (1977).

²³A. J. Jonscher, L. A. Dissado, and R. M. Hill, Phys. Status Solidi B **102**, 351 (1980).

²⁴K. L. Ngai, A. K. Jonscher, and C. T. White, Nature **277**, 185 (1979).

²⁵L. A. Dissado and R. M. Hill, Nature **279**, 685 (1979).

²⁶L. A. Dissado and R. M. Hill, Philos. Mag. B **41**, 625 (1980).